Downloaded from https://academic.oup.com/mnras//article/542/1/L103/8191231 by guest on 30 September 2025

Advance Access publication 2025 July 7

Kinematic misalignment as a driver of black hole activity in galaxies with external interactions

Sandra I. Raimundo ¹⁰, ^{1,2}★ Rogerio Riffel ¹⁰, ³ Song-lin Li, ^{4,5} Cristina Ramos Almeida ¹⁰, ^{6,7} Sandro Rembold,⁸ Rogemar A. Riffel[®],⁸ Thaisa Storchi-Bergmann,³ Marianne Vestergaard^{2,9} and José L. Tous ¹⁰

Accepted 2025 June 26. Received 2025 June 9; in original form 2024 August 7

ABSTRACT

The process of active galactic nuclei (AGN) fuelling relies on the transport of gas across several orders of magnitude in physical scale until the gas reaches the supermassive black hole at the centre of a galaxy. This work explores the role of kinematically misaligned gas in the fuelling of AGN in a sample of 4769 local galaxies from the Mapping Nearby Galaxies at Apache Point Observatory (MaNGA) survey. We investigate for the first time the relative role of external interactions and the presence of kinematic misalignment as mechanisms to explain the observed increase in AGN fraction in galaxies with large stellar to gas kinematic misalignment (>45°). Using a sample of galaxies with evidence of recent external interactions we find that there is a significantly higher fraction of AGN in those where a large stellar to gas kinematic misalignment is observed (20^{+6}_{-4}) per cent) compared with $6.2^{+0.6}_{-0.5}$ per cent in galaxies where no kinematic misalignment is observed. We determine that gas to stellar misalignment has an important role in the fraction of AGN observed, increasing the AGN fraction beyond the potential effect of external interactions. This result demonstrates the importance of misaligned structures to the fuelling of supermassive black holes.

Key words: galaxies: active – galaxies: evolution – galaxies: interactions – galaxies: kinematics and dynamics – galaxies: nuclei – galaxies: Seyfert.

1 INTRODUCTION

The process of supermassive black hole growth via gas accretion requires gas to be transported from galaxy scales to the accretion disc $(\sim 10^{16}$ cm; e.g. Morgan et al. 2010). The fuelling gas may originate from the host galaxy or from its immediate external environment. In both cases, the gas needs to lose angular momentum to be transported to the vicinity of the supermassive black hole, requiring dynamical mechanisms that are able to cause this angular momentum loss, such as galaxy interactions or large-scale bars, amongst other processes (e.g. see Shlosman, Begelman & Frank 1990; Martini 2004; Storchi-Bergmann & Schnorr-Müller 2019; Combes 2023 for reviews). This process of black hole gas fuelling is inherently connected to the powering of active galactic nuclei (AGN) and plays a decisive role in our understanding of AGN triggering mechanisms and the overall luminosity of AGN.

© The Author(s) 2025.

Although direct correlations between fuelling mechanisms and AGN are difficult to find (Martini et al. 2003), several candidate mechanisms and observational evidence to support them, have been put forward to explain the fuelling of AGN at different luminosity and redshift ranges, e.g. galaxy mergers (e.g. Ramos Almeida et al. 2011, 2012; Fischer et al. 2015; Koss et al. 2018; Araujo et al. 2023; Pierce et al. 2023; Comerford et al. 2024), bars, nuclear spirals, and gravitational torques (e.g. Shlosman, Frank & Begelman 1989; García-Burillo et al. 2005; Schnorr Müller et al. 2011, 2014; Kim & Elmegreen 2017; del Moral-Castro et al. 2020; Audibert et al. 2021; Rembold et al. 2024), stellar mass loss or interstellar medium turbulence (e.g. Davies et al. 2007; Choi et al. 2024; Riffel et al. 2024). In this work, we focus on an AGN fuelling mechanism that has recently been discovered observationally, namely that of stellar to gas kinematic misalignment (Raimundo, Malkan & Vestergaard 2023). In galaxies dominated by secular evolution, it is expected that gas and stars share a similar axis of rotation. That is in general not the case for galaxies that undergo dynamical interactions causing external gas accretion. If the amount of accreted material is significant compared

¹Physics and Astronomy, University of Southampton, Highfield, Southampton SO17 1BJ, UK

²DARK, Niels Bohr Institute, University of Copenhagen, Jagtvej 155, Copenhagen N 2200, Denmark

³Departamento de Astronomia, Instituto de Física, Universidade Federal do Rio Grande do Sul, CP 15051, 91501-970 Porto Alegre, RS, Brazil

⁴Research School of Astronomy and Astrophysics, Australian National University, Canberra, ACT 2611, Australia

⁵ARC Centre of Excellence for All-Sky Astrophysics in 3 Dimensions (ASTRO 3D), Canberra, ACT 2611, Australia

⁶Instituto de Astrofísica de Canarias, Calle Vía Láctea, s/n, 38205 La Laguna, Tenerife, Spain

⁷Departamento de Astrofísica, Universidad de La Laguna, 38206 La Laguna, Tenerife, Spain

⁸Departamento de Física, Centro de Ciências Naturais e Exatas, Universidade Federal de Santa Maria, 97105-900 Santa Maria, RS, Brazil

⁹Steward Observatory, University of Arizona, 85721 Tucson, AZ, USA

L104 S. I. Raimundo et al.

to the aligned gas and stars already present, the accreted material may end up with an angular momentum vector orientation that is distinct from that of the main stellar body of the galaxy (Haynes, Giovanelli & Chincarini 1984; Bertola, Buson & Zeilinger 1992; Sancisi et al. 2008). This can also be the consequence of kinematic misalignment of the halo itself, as has been shown by numerical simulations (Lagos et al. 2015). Notable examples of extreme angular momentum differences are polar ring/polar disc galaxies (Sérsic 1967; Schweizer, Whitmore & Rubin 1983; Bournaud & Combes 2003) or galaxies with counter-rotating cores/discs (e.g. Franx & Illingworth 1988; Rubin, Graham & Kenney 1992; Kannappan & Fabricant 2001; Pizzella et al. 2004; Sil'chenko, Moiseev & Afanasiev 2009; Raimundo et al. 2013; Bevacqua, Cappellari & Pellegrini 2022; Katkov et al. 2024). Large misalignment angles between stellar and gas motions can therefore be used to identify candidate galaxies that went through a past external accretion event, such as a major or minor merger, a galaxy flyby or gas infall from a neighbour galaxy (Bertola et al. 1992; Davis & Bureau 2016; Li et al. 2021) and to investigate the time-scale and consequence of these processes (e.g. Davis et al. 2011; Ilha et al. 2019; Khoperskov et al. 2021; Raimundo 2021; Hauschild Roier et al. 2022; Ristea et al. 2022; Xu et al. 2022; Cenci et al. 2024; Baker et al. 2025).

Observations point towards a connection between stellar to gas misalignment and a higher fraction of AGN activity. Raimundo et al. (2023) have shown that galaxies with large kinematic misalignment angles (>45°) have a higher fraction of AGN than galaxies without misalignment, suggesting that stellar to gas kinematic misalignment and/or the external accretion event that originated it, is connected with the fuelling of AGN. Black hole fuelling requires gas and dynamical mechanisms to promote the loss of angular momentum, and both these conditions can be met in galaxies with large misalignment. First, external accretion events provide a supply of gas to the host galaxy, which is potentially significant for earlytype galaxies without a large reservoir of native gas (Simões Lopes et al. 2007; Davies et al. 2014; Raimundo et al. 2017; Khim et al. 2020). Secondly, it has been shown from simulations that misaligned structures (stellar/stellar or stellar/gas misalignment) promote the loss of angular momentum and the flow of gas towards the centre of the galaxy, via for example stellar torques, shocks in the gas or dynamical friction (Thakar & Ryden 1996; Negri, Ciotti & Pellegrini 2014; van de Voort et al. 2015; Capelo & Dotti 2017; Taylor, Federrath & Kobayashi 2018; Starkenburg et al. 2019; Duckworth et al. 2020; Khoperskov et al. 2021), with recent observational evidence supporting that hypothesis (Raimundo 2021; Zhou et al. 2022; Raimundo et al. 2023).

Since kinematic misalignment is very often a consequence of an external accretion event, the two factors (external gas supply and kinematic misalignment) can be linked when investigating their effect on AGN. While they may both contribute to the observed increase in AGN (Raimundo et al. 2023), it is unclear if the isolated effect of kinematic misalignment makes a significant contribution to increase the fraction of AGN. This is particularly important since mergers of galaxies, which cause $\sim 10-20$ per cent of misalignments in massive galaxies $(M_* > 10^{10} M_{\odot})$ (Baker et al. 2025), have been observed to be connected with higher fractions of AGN (e.g. Comerford et al. 2024; Rembold et al. 2024, for the MaNGA sample). To answer this question, we investigate whether the presence of misalignment has a prevalent effect in the increase of AGN fraction in galaxies with both signatures of external interactions and stellar to gas misalignment. In Section 2, we describe the data and the methods used to determine kinematic position angles, to identify AGN and to identify galaxies with recent interactions. In Section 3, we show how the AGN fraction varies as a function of misalignment angle, and discuss the driving mechanism for the observed increased fraction of AGN in galaxies with strong kinematic misalignment.

2 DATA ANALYSIS

We used observations from the Data Release 17 of the Mapping Nearby Galaxies at Apache Point Observatory (MaNGA) optical integral field unit survey of $\sim 10~000$ local galaxies (Bundy et al. 2015; Abdurro'uf et al. 2022). The survey covers a redshift range of 0.01 < z < 0.15 and stellar masses $M_{\star} > 10^9 M_{\odot}$. In this work, we use the MaNGA 2D maps of gas and stellar properties as analysed and compiled in the form of multiple extension fits files (MEGACUBES)¹ and presented in detail by Riffel et al. (2023).

2.1 Measurement of kinematic position angles

The global kinematic position angles represent the mean motion of the stars (PA_{stellar}) and of the gas (PA_{gas}), and are determined from two-dimensional maps of stellar and gas velocity, respectively. The position angle is defined as the angle between the north and the line that connects the absolute maxima of the velocity. To calculate the position angles we follow the same approach as in Raimundo et al. (2023), applying the FIT_KINEMATIC_PA algorithm (Krajnović et al. 2006) to the maps of ionized gas velocity (obtained from measuring the velocity of the H α emission lines) and stellar velocity from the MEGACUBES distribution (Riffel et al. 2023).

In this work, we are interested in the difference between the direction of motion of stars and gas in a galaxy as projected in the sky plane, i.e. how misaligned the stellar and gas rotation axes are. The misalignment angle (ΔPA) for each galaxy is calculated from the difference between the global stellar and gas kinematic angles: $\Delta PA = |PA_{stellar} - PA_{gas}|$ and can vary between 0° (perfect alignment) and 180° (counter-rotation). We would like to highlight that these angles reflect global gas and stellar motions measured at scales of hundreds of parsecs to kiloparsecs, and not local small-scale variations. To determine ΔPA we require that both $PA_{stellar}$ and PA_{gas} can be measured accurately. Our quality cuts are similar to those implemented by Raimundo et al. (2023): we only use velocity map pixels where the uncertainties in the velocities are lower than 30 km s^{-1} , and require the uncertainty on the measured ΔPA to be lower that 30°. We also require a minimum of 20 good pixels to determine the stellar or gas PA. In total, we have a sample of 4769 galaxies for which the misalignment angle was determined. This is our parent sample. Within this sample, 87 per cent are late-type galaxies and 13 per cent are early-type galaxies, according to the visual morphology classification of Vázquez-Mata et al. (2022).

2.2 AGN identification

To identify AGN, we combine two different approaches. The first is the AGN optical identification based on the spatially resolved Baldwin, Phillips & Terlevich (Baldwin, Phillips & Terlevich 1981) diagrams as described by Raimundo et al. (2023). The second is the AGN identification by Comerford et al. (2024) using multi-wavelength observations and catalogues. The AGN classification of Raimundo et al. (2023) uses spatially resolved narrow emission line ratios to identify AGN, and more details can be found in that work. The Comerford et al. (2024) AGN identification includes broad

¹manga.linea.org.br

emission line AGN detected in the Sloan Digital Sky Survey (SDSS), AGN classified in infrared (Wide-Field Infrared Survey Explorer -WISE), radio (Faint Images of the Radio Sky at Twenty cm – FIRST) and X-ray (Swift Burst Alert Telescope – Swift/BAT) catalogues. We combine these two samples of AGN and match them to the sample of 4769 galaxies for which the misalignment angle was determined. Our final sample of AGN with measured ΔPA contains a total of 274 AGN (out of N = 4769 galaxies with measured kinematic angles, i.e. an AGN fraction of 5.7 per cent). Among the AGN sample, 81 per cent of them are in late-type galaxies while 19 per cent are in early-type galaxies. The stellar mass range of the AGN host galaxies is distributed from $M_{\star} \sim 10^9$ – $10^{11}~M_{\odot}$ with a peak at $\sim 10^{10.4} M_{\odot}.$ The AGN [O III] luminosity range is typically $L_{OIII} \sim 10^{39}-10^{41.5}$ erg s⁻¹, which indicates that these are low to moderate luminosity AGN (Winiarska et al. 2025). The low-luminosity range of the AGN supports previous findings (Raimundo et al. 2023), that the gas kinematic misalignment observed in AGN hosts is not driven by potential AGN outflows (Ilha et al. 2019; Khoperskov et al. 2021; Raimundo et al. 2023). This is because of the observed trend between outflow size and AGN luminosity (e.g. Kim et al. 2023). In addition to the AGN selection outlined above, we also used, as a comparison, the AGN identification presented by Rembold et al. (2017) and Riffel et al. (2023) based on the diagnostic diagrams of Baldwin, Phillips & Terlevich (Baldwin et al. 1981) and that of the equivalent width of $H\alpha$ versus [N II]/ $H\alpha$ (WHAN) of Cid Fernandes et al. (2010). The results will be discussed in Section 3.

2.3 Signatures of galaxy interactions

To identify galaxies that underwent recent interactions in the MaNGA sample, we combine two methods: the visual classification of Li et al. (2021) for MaNGA galaxies that show evidence of a past interaction, and the machine learning identification of major and minor mergers from Nevin et al. (2023) as used by Comerford et al. (2024) in their analysis of MaNGA. Li et al. (2021) used deep images from the Dark Energy Spectroscopic Instrument (DESI) Legacy Imaging Surveys (Dey et al. 2019) to visually search for evidence of past interactions in the MaNGA sample. We use their sample of 538 galaxies with merging features or evidence of strong interaction with companions identified in the MaNGA sample. such as tidal features, distortions/asymmetries or shells. From the sample of Comerford et al. (2024) we use the galaxies that have a probability above 50 per cent of being either major mergers or minor mergers. Out of our initial sample of 4769 MaNGA galaxies with well measured kinematic angles, 1780 galaxies show evidence of interactions according to either one of the methods described above (Li et al. 2021 or Comerford et al. 2024). Out of 1780 galaxies with interactions, 1662 are selected using the Comerford et al. 2024 method. An extra 132 galaxies are identified in the Li et al. (2021) catalogue only. Within the sample of 1780 galaxies, 91 per cent are late-type galaxies and 9 per cent are early-type galaxies, according to the visual morphology classification of Vázquez-Mata et al. (2022). Since the identification of interactions relies on photometric features, it means that we are identifying relatively recent interactions, before the features evolved and became too faint to be identified.

3 RESULTS AND DISCUSSION

In the following sections, we investigate the trend between AGN fraction and misalignment angle for the MaNGA sample and study if the same trend is found in the sub-sample of 1780 MaNGA galaxies that have signatures of past interactions.

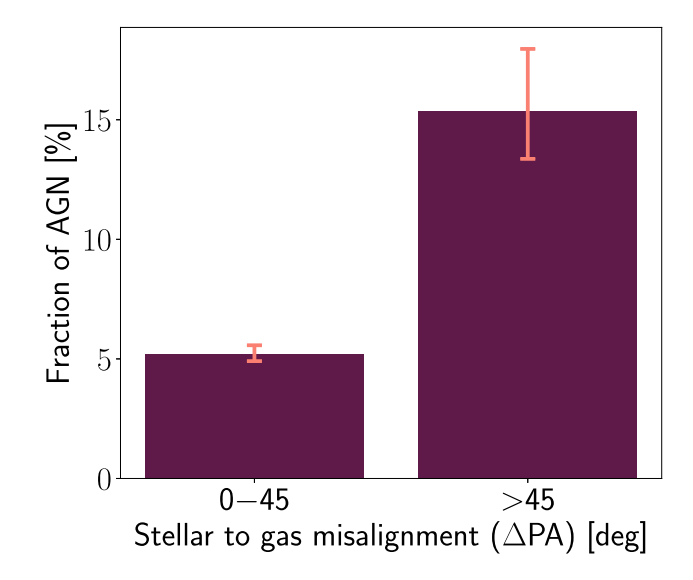


Figure 1. Fraction of AGN as a function of stellar to gas kinematic misalignment (Δ PA in degrees) for the galaxies in the MaNGA survey. Galaxies with significant kinematic misalignment (Δ PA $\geq 45^{\circ}$) show a higher fraction of AGN: 15^{+2}_{-2} per cent compared with $5.2^{+0.4}_{-0.3}$ per cent for the galaxies with Δ PA $< 45^{\circ}$. The error bars indicate the 68 per cent confidence intervals calculated using the beta distribution quantile technique for a binomial population (Cameron 2011).

3.1 Fraction of AGN in galaxies with misalignment

To investigate if the fraction of AGN changes for galaxies with and without a significant misalignment between stellar and gas kinematics, we follow the method of Raimundo et al. (2023). We start with the full sample of MaNGA galaxies for which the measurement of stellar and gas kinematic angles was possible (N = 4769 galaxies). We then divide the sample into two groups: those with $\Delta PA < 45^{\circ}$, which are galaxies for which stellar and gas kinematic angles are likely aligned within the uncertainties (N = 4522), and those with $\Delta PA \ge 45^{\circ}$, which are galaxies for which a significant misalignment is observed (N = 247). In Fig. 1, we show the fraction of AGN in these two misalignment bins. We find an AGN fraction of $5.2_{-0.3}^{+0.4}$ per cent for galaxies with $0^{\circ} \leq \Delta PA < 45^{\circ}$ and a fraction of 15^{+2}_{-2} per cent for galaxies with $\Delta PA \ge 45^{\circ}$. It is clear that there is a significantly higher (>3 σ level) fraction of AGN in galaxies with misaligned gas and stars for the MaNGA sample, similar to what is found for the SAMI (Sydney-AAO Multi-object Integral field spectrograph) survey, which covers a similar redshift range but has a smaller galaxy sample size (Raimundo et al. 2023). We also observe an increased fraction of AGN if we consider polar galaxies ($\Delta PA \sim 90^{\circ}$) or counter-rotating galaxies ($\Delta PA \sim 180^{\circ}$) separately. In Fig. 2, we show the same sample but divided into 20° bins. While there are fewer galaxies per bin, this figure is useful to illustrate that the main differences in AGN fraction occurs for $\Delta PA \gtrsim 60^{\circ}$.

It is known that early-type galaxies have a higher fraction of kinematic misalignment than late types (e.g. Bertola et al. 1991; Pizzella et al. 2004; Davis et al. 2011; Raimundo et al. 2023). To check that the trend that we observe is not driven by a preference of AGN for early-type hosts, we use the T-Type (de Vaucouleurs 1959) visual morphology classifications as presented in Vázquez-Mata et al. (2022) to investigate the distribution of AGN host morphologies. The T-Type values can be related to the Hubble classification in that T-Type values <1 correspond to early-type galaxies and T-Type values ≥1 to late-type galaxies. We show our results in Fig. 3, with

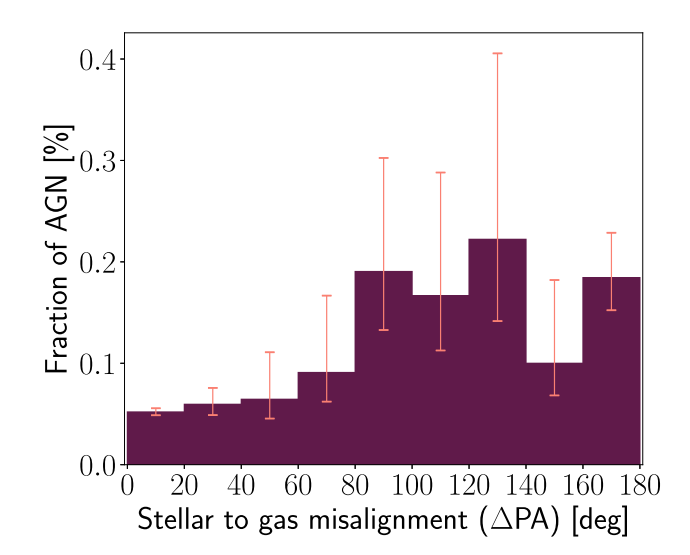


Figure 2. Fraction of AGN as a function of stellar to gas kinematic misalignment (Δ PA in degrees) for the galaxies in the MaNGA survey, divided into 20° bins. This figure is similar to Fig. 1 but with smaller number statistics due to the reduced number of galaxies per bin. The error bars indicate the 68 per cent confidence intervals calculated using the beta distribution quantile technique for a binomial population (Cameron 2011).

a histogram of AGN host numbers as a function of T-Type. The orange histogram shows early-type hosts, while the blue histogram shows late-type hosts. Within the sample of MaNGA AGN galaxies with measured stellar and gas kinematic angles, most hosts are late types. We also carry out the quantitative exercise of estimating the difference in AGN fraction between each bin: $\Delta PA < 45^{\circ}$ and ΔPA > 45°, that would be expected from having the combined effect of a higher fraction of AGN in early-type galaxies and a higher fraction of early-type galaxies with misalignment. Within the 4522 aligned galaxies of the parent sample, 90 per cent are late type and 10 per cent early type. Within the 247 misaligned galaxies there are 38 per cent late type and 62 per cent early types. In the overall MaNGA sample with or without measured kinematic angles the fraction of AGN in late types is 5 per cent and in early types 7 per cent. Based on these values and without any additional trend, the expected fraction of AGN in $\Delta PA < 45^{\circ}$ would be ~ 5 per cent and in $\Delta PA \ge 45^{\circ}$ would be \sim 6 per cent, resulting in a difference of \sim 1 per cent, which is a much smaller difference than what we see in our sample (\sim 9–10 per cent; Fig. 1). Fig. 3 and the quantitative exercise above support the argument that the trend for a higher fraction of AGN in misaligned galaxies is not due to a double correlation between AGN and earlytype morphology and early-type morphology and misalignment but needs an additional effect which our work argues is the presence of misaligned gas.

3.2 Driving mechanism – galaxy interactions or misaligned gas?

In this work, we want to separate the effect of external interactions from kinematic misalignment in driving the increase in AGN fraction. Kinematic misalignment is the result of external accretion but not all external accretion and interactions will result in a large kinematic misalignment. Depending on the configuration, the external inflow of material may end up in kinematic alignment ($\Delta PA = [0^{\circ} - 45^{\circ}]$) or relaxing into kinematic alignment with a particular time delay after the interaction. For example, polar disc galaxies are found

to settle into co/counter-rotation within 1-3 Gyr (Khoperskov et al. 2021). Kinematic misalignment can also be longer lived than the time during which morphological signatures of interactions are observed (Starkenburg et al. 2019; Ebrová, Łokas & Eliášek 2021). Therefore, galaxies may show kinematic misalignment but no signatures of the interaction that generated it. To determine which of the mechanisms is dominant in increasing the fraction of active black holes, we select the sample of MaNGA galaxies with signatures of recent interactions as our parent sample, finding a total of 1780 galaxies (1710 with $0^{\circ} \leq \Delta PA < 45^{\circ}$ and 70 with $\Delta PA \geq 45^{\circ}$). These galaxies may have had different types of external interactions, therefore in this work we do not establish the role of a particular external interaction but analyse all types of external interactions as a whole. We then determine the fraction of AGN on the sub-samples of galaxies with aligned and misaligned stellar to gas kinematics. If external accretion (through some form of interaction or merger activity) was the most important factor and gas kinematical misalignment is irrelevant, then we should expect to see no statistical difference in the ΔPA distribution for the galaxies with an AGN (for this galaxy sub-set with evidence of interactions). In Fig. 4, we show the fraction of AGN as a function of kinematic misalignment angle. We find an AGN fraction of $6.2_{-0.5}^{+0.6}$ per cent for galaxies with $0^{\circ} \leq \Delta PA < 45^{\circ}$ and a fraction of 20^{+6}_{-4} per cent for galaxies with $\Delta PA \ge 45^{\circ}$, different by $\sim 3\sigma$. A difference is also found between the two populations (albeit with smaller number statistics) if we use only the Riffel et al. (2023) sample of AGN [which includes a WHAN diagnostic (Cid Fernandes et al. 2010)] or only the Comerford et al. 2024 AGN sample. With our main sample shown in Fig. 4, it is clear that even within the sample of galaxies with interactions (which includes major/minor mergers and different stages of interaction), there is a significantly higher fraction of AGN in galaxies with misaligned gas and stars ($\Delta PA > 45^{\circ}$) than for kinematically aligned gas and stars. This shows that the presence of misalignment is connected with an additional increase in the fraction of AGN, being a potentially important ingredient for the activation of the black hole.

Comerford et al. (2024) recently found that among galaxies with signatures of past major or minor mergers in MaNGA, there is an increased number of AGN. Comparing Figs 1 and 4, we find a tentative increase in the overall fraction of AGN in all galaxies (aligned and misaligned combined) from 5.1 per cent in the initial sample to 6.8 per cent in the sample of galaxies with signatures of past interactions. Both samples consist of galaxies for which stellar and gas kinematic angles can be determined, and therefore neither is an unbiased sample. In any case, the increased fractions we observe is in line with the results of Comerford et al. (2024).

We test whether the trend we observe in Fig. 4 is also present if we split the sample by stellar mass or morphology. The main limitation we have is the small number statistics, which affect the significance of the results. In any case, we find a difference of $> 2.5\sigma$ between the two populations even if we split the sample into low- and high-stellar masses (using a threshold of $\log(M_*/\mathrm{M}_\odot) = 9.5$, 10, or 10.5), showing that the trend we observe is not driven by differences in stellar mass. We also find evidence that the trend is still present when the sample is split into spirals versus ellipticals and S0s, suggesting that the trend we see is not driven by morphology.

Previous work has shown a connection between the presence of kinematically misalignment and the fraction of galaxies with AGN, but did not separate the effect of external interactions and external gas accretion from kinematic misalignment, due to the limited sample size (Raimundo et al. 2023). With our MaNGA sample we show that even within the sample of galaxies with evidence for interactions, there is an additional increase in the fraction of galaxies

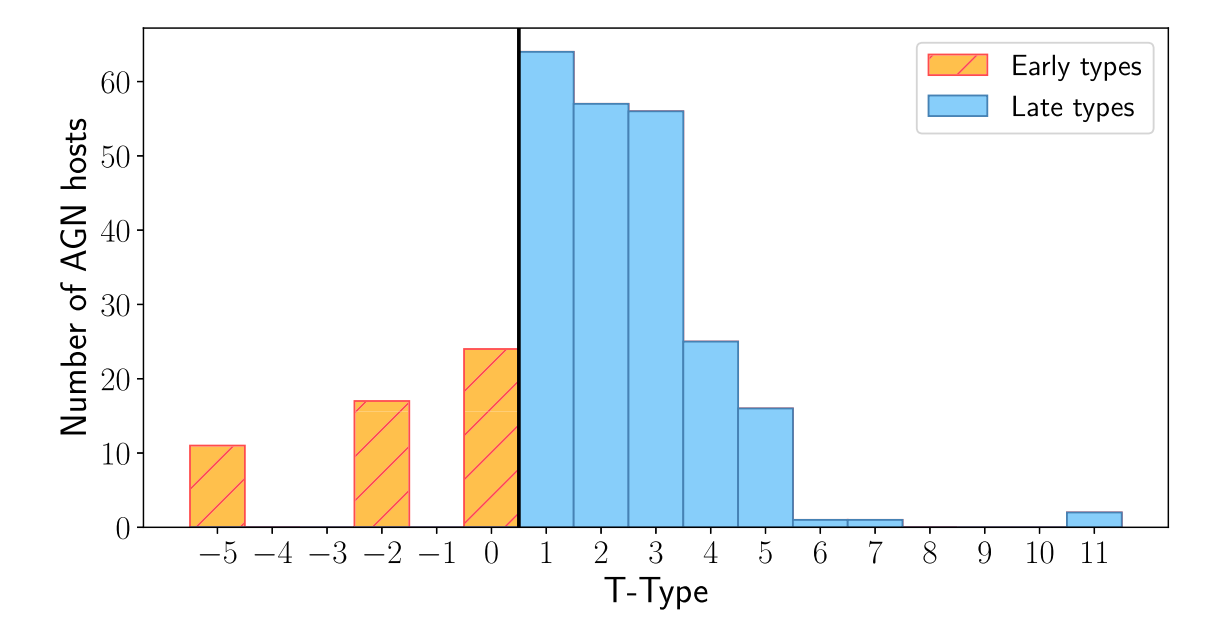


Figure 3. Distribution of AGN host morphology for the 274 AGN in our sample. The morphology is given by the T-Type morphology indicator which takes on discrete integer values (Vázquez-Mata et al. 2022). Each bin is centred at the specific discrete value in T-Type with a width of 0.5 for visualization purposes. The orange hatched histogram shows the AGN host galaxies that are early-type galaxies (T-Type <1), while the blue histogram shows the AGN host galaxies that are late types (T-Type ≥ 1).

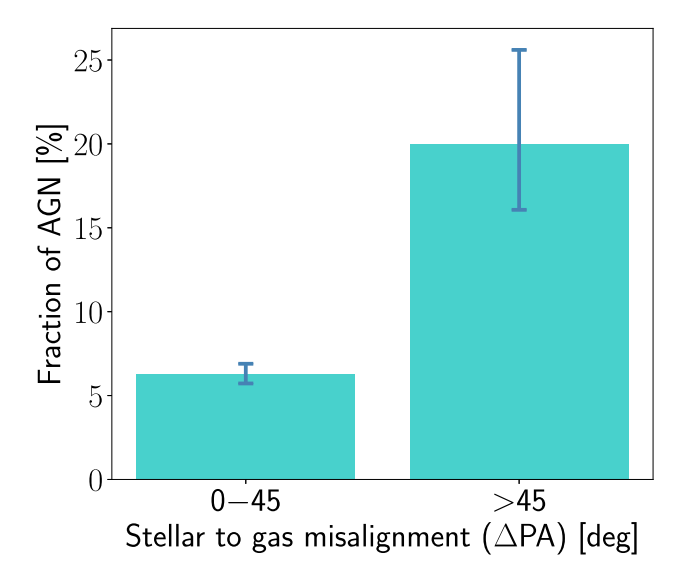


Figure 4. Fraction of AGN as a function of stellar to gas kinematic misalignment (ΔPA in degrees) for the galaxies in the MaNGA survey that show signatures of a past interaction. Galaxies with significant kinematic misalignment ($\Delta PA \geq 45^{\circ}$) show a higher fraction of AGN, indicating that misalignment is a driving mechanism for the increased fraction of AGN and not only due to a dynamical interaction, such as a merger. The relative fractions are 20^{+6}_{-4} per cent for galaxies with $\Delta PA \geq 45^{\circ}$ compared to $6.2^{+0.6}_{-0.5}$ per cent for the galaxies with $\Delta PA < 45^{\circ}$. The error bars indicate the 68 per cent confidence intervals calculated using the beta distribution quantile technique for a binomial population (Cameron 2011).

with misalignment that host an AGN. The relative difference in AGN fraction in the interacting galaxy sample is similar to what is seen in the full sample (Fig. 1). This shows that while galaxy interactions, such as mergers, may be important for the increase in observed AGN fraction (e.g. Comerford et al. 2024), the dominant

mechanism behind the difference in AGN fraction observed in this work [and likely for SAMI (Raimundo et al. 2023)], is the presence of kinematically misaligned structures.

Kinematically misaligned structures can only be produced via the external accretion of gas, and therefore galaxy interactions are fundamental to creating the misalignment in the first place. What we show in our work is that for interactions that end up in kinematic misalignment (as opposed to aligned rotation of gas and stars), black holes are more likely in an active phase. This finding indicates that kinematic misalignment plays a major role in the observed fraction of active black holes after an external accretion event.

4 CONCLUSIONS

In this work, we investigate the driving mechanism for the observed higher fraction of AGN residing in galaxies with misaligned gas-to-stellar kinematic axes. We measure a higher fraction of AGN (15^{+2}_{-2}) per cent) in MaNGA galaxies with strong misalignment between gas and stellar rotation ($\Delta PA \geq 45^{\circ}$) than in galaxies with aligned gas and stellar rotation ($5.2^{+0.4}_{-0.3}$ per cent). This result is in line with what was previously found for the smaller sample of galaxies in the SAMI survey (Raimundo et al. 2023), and shows a connection between the presence of kinematically misaligned gas and a higher fraction of observed black hole activity.

Kinematically misaligned gas is the consequence of an external accretion event but not all external accretion events result in strongly misaligned stellar to gas kinematics. We therefore investigate for the first time whether the observed increase in the fraction of AGN activity is also driven by the presence of misaligned gas or simply by the external accretion event, irrespective of whether the gas ends up aligned or misaligned. We find that the overall fraction of AGN in interacting galaxies (i.e. those with visual signatures of a past external accretion event) is slightly higher than in the total sample that contains galaxies with and without past interactions. Most importantly, within the sample with evidence for interactions,

we still find a higher fraction of AGN in galaxies with misaligned gas (20^{+6}_{-4} per cent for $\Delta PA \geq 45^{\circ}$ versus $6.2^{+0.6}_{-0.5}$ per cent for $\Delta PA < 45^{\circ}$). This result indicates that even when comparing galaxies with recent interactions, the misalignment between stellar and gas rotation is associated with an increase of the AGN fraction. The conclusion of this work is that gas-to-stellar kinematic misalignment is driving the increase in AGN fraction, even within the sample where all galaxies had recent external interactions. This result shows the importance of kinematically misaligned structures to the loss of gas angular momentum and to the fuelling of supermassive black holes.

ACKNOWLEDGEMENTS

We would like to thank the referee for their careful reading of the manuscript and constructive comments. This work was supported by the Science and Technology Facilities Council (STFC) of the UK Research and Innovation via grant reference ST/Y002644/1 and by the European Union's Horizon 2020 research and innovation programme under the Marie Sklodowska-Curie grant agreement No 891744 (SIR). RR thanks Conselho Nacional de Desenvolvimento Científico e Tecnológico (CNPq, Proj. 311223/2020-6, 304927/2017-1, and 400352/2016-8), Fundação de amparo à pesquisa do Rio Grande do Sul (FAPERGS, Proj. 16/2551-0000251-7 and 19/1750-2), Coordenação de Aperfeiçoamento de Pessoal de Nível Superior (CAPES, Proj. 0001). RAR acknowledges the support from CNPq (Proj. 303450/2022-3, 403398/2023-1, and 441722/2023-7), FAPERGS (Proj. 21/2551-0002018-0), and CAPES (Proj. 88887.894973/2023-00). MV gratefully acknowledges financial support from the Independent Research Fund Denmark via grant number DFF 8021-00130. CRA acknowledges support from the Agencia Estatal de Investigación of the Ministerio de Ciencia, Innovación y Universidades (MCIU/AEI) under the grant 'Tracking active galactic nuclei feedback from parsec to kiloparsec scales', with reference PID2022-141105NB-I00 and the European Regional Development Fund (ERDF).

This research has made use of MaNGA data from SDSS IV. Funding for the Sloan Digital Sky Survey IV has been provided by the Alfred P. Sloan Foundation, the U.S. Department of Energy Office of Science, and the Participating Institutions. SDSS acknowledges support and resources from the Center for High-Performance Computing at the University of Utah. The SDSS web site is www.sdss4.org. This research has made use of the VizieR catalogue access tool, CDS, Strasbourg, France (DOI: 10.26093/cds/vizier), Ochsenbein, Bauer & Marcout (2000). This research made use of ASTROPY, http://www.astropy.org a community-developed core PYTHON package for astronomy (Astropy Collaboration 2013).

DATA AVAILABILITY

The MaNGA MEGACUBES used in this work are publicly available through a web interface at https://manga.linea.org.br/ and https://manga.if.ufrgs.br/. The data underlying this article will be shared on reasonable request to the corresponding author.

REFERENCES

Abdurro'uf et al., 2022, ApJS, 259, 35 Araujo B. L. C., Storchi-Bergmann T., Rembold S. B., Kaipper A. L. P., Dall'Agnol de Oliveira B., 2023, MNRAS, 522, 5165 Astropy Collaboration, 2013, A&A, 558, A33 Audibert A. et al., 2021, A&A, 656, A60

Baker M. K., Davis T. A., van de Voort F., Ruffa I., 2025, MNRAS, 541, 494

Baldwin J. A., Phillips M. M., Terlevich R., 1981, PASP, 93, 5
Bertola F., Bettoni D., Danziger J., Sadler E., Sparke L., de Zeeuw T., 1991, ApJ, 373, 369
Bertola F., Buson L. M., Zeilinger W. W., 1992, ApJ, 401, L79
Bevacqua D., Cappellari M., Pellegrini S., 2022, MNRAS, 511, 139

Bournaud F., Combes F., 2003, A&A, 401, 817

Bundy K. et al., 2015, ApJ, 798, 7

Cameron E., 2011, PASA, 28, 128

Capelo P. R., Dotti M., 2017, MNRAS, 465, 2643

Cenci E., Feldmann R., Gensior J., Bullock J. S., Moreno J., Bassini L., Bernardini M., 2024, ApJ, 961, L40

Choi E., Somerville R. S., Ostriker J. P., Hirschmann M., Naab T., 2024, ApJ, 964, 54

Cid Fernandes R., Stasińska G., Schlickmann M. S., Mateus A., Vale Asari N., Schoenell W., Sodré L., 2010, MNRAS, 403, 1036

Combes F., 2023, Galaxies, 11, 120

Comerford J. M. et al., 2024, ApJ, 963, 53

Davies R. I., Müller Sánchez F., Genzel R., Tacconi L. J., Hicks E. K. S., Friedrich S., Sternberg A., 2007, ApJ, 671, 1388

Davies R. I. et al., 2014, ApJ, 792, 101

Davis T. A., Bureau M., 2016, MNRAS, 457, 272

Davis T. A. et al., 2011, MNRAS, 417, 882

de Vaucouleurs G., 1959, Handbuch der Physik, 53, 311

del Moral-Castro I. et al., 2020, A&A, 639, L9

Dey A. et al., 2019, AJ, 157, 168

Duckworth C., Starkenburg T. K., Genel S., Davis T. A., Habouzit M., Kraljic K., Tojeiro R., 2020, MNRAS, 495, 4542

Ebrová I., Łokas E. L., Eliášek J., 2021, A&A, 647, A103

Fischer T. C., Crenshaw D. M., Kraemer S. B., Schmitt H. R., Storchi-Bergmann T., Riffel R. A., 2015, ApJ, 799, 234

Franx M., Illingworth G. D., 1988, ApJ, 327, L55

García-Burillo S., Combes F., Schinnerer E., Boone F., Hunt L. K., 2005, A&A, 441, 1011

Hauschild Roier G. R. et al., 2022, MNRAS, 512, 2556

Haynes M. P., Giovanelli R., Chincarini G. L., 1984, ARA&A, 22, 445

Ilha G. S. et al., 2019, MNRAS, 484, 252

Kannappan S. J., Fabricant D. G., 2001, AJ, 121, 140

Katkov I. Y., Gasymov D., Kniazev A. Y., Gelfand J. D., Rubtsov E. V., Chilingarian I. V., Sil'chenko O. K., 2024, ApJ, 962, 27

Khim D. J. et al., 2020, ApJ, 894, 106

Khoperskov S. et al., 2021, MNRAS, 500, 3870

Kim W.-T., Elmegreen B. G., 2017, ApJ, 841, L4

Kim C., Woo J.-H., Luo R., Chung A., Baek J., Le H. A. N., Son D., 2023, ApJ, 958, 145

Koss M. J. et al., 2018, Nature, 563, 214

Krajnović D., Cappellari M., de Zeeuw P. T., Copin Y., 2006, MNRAS, 366, 787

Lagos C. d. P., Padilla N. D., Davis T. A., Lacey C. G., Baugh C. M., Gonzalez-Perez V., Zwaan M. A., Contreras S., 2015, MNRAS, 448, 1271

Li S.-l. et al., 2021, MNRAS, 501, 14

Martini P., 2004, in Storchi-Bergmann T., Ho L. C., Schmitt H. R., eds, IAU Symp. Vol. 22, The Interplay Among Black Holes, Stars and ISM in Galactic Nuclei. Cambridge Univ. Press, Cambridge, p. 235

Martini P., Regan M. W., Mulchaey J. S., Pogge R. W., 2003, ApJ, 589, 774
 Morgan C. W., Kochanek C. S., Morgan N. D., Falco E. E., 2010, ApJ, 712, 1129

Negri A., Ciotti L., Pellegrini S., 2014, MNRAS, 439, 823

Nevin R., Blecha L., Comerford J., Simon J., Terrazas B. A., Barrows R. S., Vázquez-Mata J. A., 2023, MNRAS, 522, 1

Ochsenbein F., Bauer P., Marcout J., 2000, A&AS, 143, 23

Pierce J. C. S. et al., 2023, MNRAS, 522, 1736

Pizzella A., Corsini E. M., Vega Beltrán J. C., Bertola F., 2004, A&A, 424, 447

Raimundo S. I., 2021, A&A, 650, A34

Raimundo S. I., Davies R. I., Gandhi P., Fabian A. C., Canning R. E. A., Ivanov V. D., 2013, MNRAS, 431, 2294

Raimundo S. I., Davies R. I., Canning R. E. A., Celotti A., Fabian A. C., Gandhi P., 2017, MNRAS, 464, 4227

Raimundo S. I., Malkan M., Vestergaard M., 2023, Nat. Astron., 7, 463Ramos Almeida C., Tadhunter C. N., Inskip K. J., Morganti R., Holt J., Dicken D., 2011, MNRAS, 410, 1550

Ramos Almeida C. et al., 2012, MNRAS, 419, 687

Rembold S. B. et al., 2017, MNRAS, 472, 4382

Rembold S. B. et al., 2024, MNRAS, 527, 6722

Riffel R. et al., 2023, MNRAS, 524, 5640

Riffel R. et al., 2024, MNRAS, 531, 554

Ristea A. et al., 2022, MNRAS, 517, 2677

Rubin V. C., Graham J. A., Kenney J. D. P., 1992, ApJ, 394, L9

Sancisi R., Fraternali F., Oosterloo T., van der Hulst T., 2008, A&AR, 15, 189

Schnorr Müller A., Storchi-Bergmann T., Riffel R. A., Ferrari F., Steiner J. E., Axon D. J., Robinson A., 2011, MNRAS, 413, 149

Schnorr-Müller A., Storchi-Bergmann T., Nagar N. M., Ferrari F., 2014, MNRAS, 438, 3322

Schweizer F., Whitmore B. C., Rubin V. C., 1983, AJ, 88, 909

Sérsic J. L., 1967, ZAp, 67, 306

Shlosman I., Frank J., Begelman M. C., 1989, Nature, 338, 45

Shlosman I., Begelman M. C., Frank J., 1990, Nature, 345, 679

Sil'chenko O. K., Moiseev A. V., Afanasiev V. L., 2009, ApJ, 694, 1550
Simões Lopes R. D., Storchi-Bergmann T., de Fátima Saraiva M., Martini P.,
2007, ApJ, 655, 718

Starkenburg T. K., Sales L. V., Genel S., Manzano-King C., Canalizo G., Hernquist L., 2019, ApJ, 878, 143

Storchi-Bergmann T., Schnorr-Müller A., 2019, Nat. Astron., 3, 48

Taylor P., Federrath C., Kobayashi C., 2018, MNRAS, 479, 141

Thakar A. R., Ryden B. S., 1996, ApJ, 461, 55

van de Voort F., Davis T. A., Kereš D., Quataert E., Faucher-Giguère C.-A., Hopkins P. F., 2015, MNRAS, 451, 3269

Vázquez-Mata J. A. et al., 2022, MNRAS, 512, 2222

Winiarska M. W., Raimundo S. I., Davis T. A., Riffel R., Shankar F., Wiseman P., 2025, MNRAS, 538, 1191

Xu H. et al., 2022, MNRAS, 511, 4685

Zhou Y. et al., 2022, MNRAS, 515, 5081

This paper has been typeset from a TFX/LATFX file prepared by the author.